4ème Conférence Internationale des Energies Renouvelables (CIER-2016)
Proceedings of Engineering and Technology – PET
Vol.17 , pp. 102 - 108

Average Model of a DC/DC Converter used in Battery Storage System

Abdessattar Jendoubi[#1], Najib Fnaiech [*2], Faouzi Bacha[#3]

[#] *LISI, INSAT, University of Carthage*

INSAT Centre Urbain Nord BP 676 - 1080 Tunis Cedex, Tunis 1080

[1]Jendoubiabdessattar@gmail.com

[3]Faouzi.Bacha@esstt.rnu.tn

[2]Fneichnejib@yahoo.fr

Abstract— **To optimize a battery storage photovoltaic system, it is necessary to exploiting continuously the maximum power generated by photovoltaic array under variation in the weather conditions. This exploitation overcomes the problem of mismatch between the photovoltaic generator and nonlinear load (battery). In this paper, we present a system transferring power from photovoltaic module to a battery through an adaptation method based on an average model of a DC/DC buck converter. This average model is employed to overcome the long-term simulations problem and effects of states of charge to electrochemical load. It is controlled by a simple curve fitting technique method. The high performance and the effectiveness of the average model DC/DC converter and appropriate control method are investigate through the Matlab Simulink software, in order to confirming the optimization of automatic charging system during a real irradiation day.**

Keywords— **Average model dc-dc buck converter, Maximum power point tracking algorithm, Curve fitting technique method, Electrochemical load, Lead acid battery.**

I. Introduction

The reduction of greenhouse effect, generated by fossil fuels, motivates many scientists to have recourse the renewable energies not polluting. Among these energies one finds this photovoltaic (PV) whose electrical energy is produced by PV panels [1]-[5].

However, two principal constraints constrain the operation of these systems. The first is solar cell conversion efficiency which does not exceed 20% of the received energy. The second concern the critical interactions between the sources and load (battery) which is nonlinear. This nonlinearity is due to:

• The instability of irradiation during a day because of weather conditions variable.

• The nonlinear characteristics of electrochemical storage battery [4].

One finds in literature a few results concerning the interaction optimization between the photovoltaic sources and loads. Particularly, the work in [7] has treated the solar array as a current source; it has tracker the maximum power points to optimize the operation to system. The principle of energy conservation was used in this work and it was implemented in a digital signal processor. The experimental results show excellent performance, but it doesn't present a battery model allowing us to have a real dynamics of the energy storage system. Similarly the work in [8] focuses on the control of battery charging evolution but without consider of the effects of irradiation instability on the dynamic operation of the system.

Firstly, this work investigates how the irradiation affects the performance of solar power generation. Secondly, we discusses the topology of the power interface used, the control method to exploit the maximum power generated by photovoltaic array and dealer us the dynamic battery model (Electrochemical load). Finally, the simulations results of energy storage system during a real day will be illustrated

II. Description and Modelling of the Battery Storage Photovoltaic System

In this study, battery storage photovoltaic system is composed by these following subsystems:

- A PVG constituted with 72 solar cells in series.
- Variable controller of tracking power point maximal (MPPT).
- DC/DC converter.
- Battery model.

This system can be described by Fig. 1

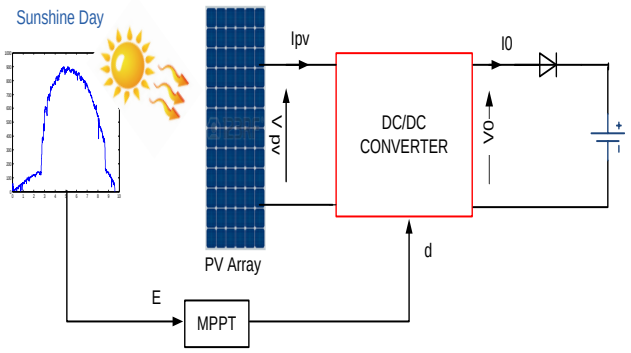

Fig. 1 Diagram of the photovoltaic battery-storage system

The following sections present the modeling and characteristic of each subsystem of battery storage photovoltaic system.

ISSN 2356-5608

A. *Photovoltaic Generator modeling and characteristics analysis*

The electrical model and parameters of solar cell are illustrated in Fig. 2. This model is useful to simulate the PV array behaviour with Matlab-Simulink Software.

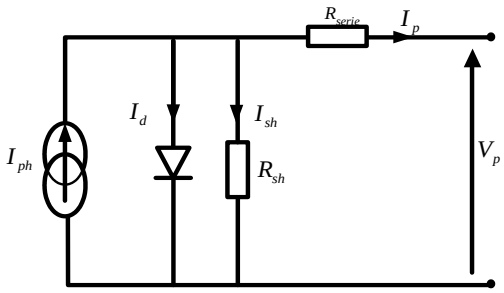

Fig. 2. Photovoltaic cell equivalent circuit

The relationship between the PV cell output current and voltage is given by [1].

$$I_p = I_{ph} - I_s\left[\exp\left(\frac{V_p + R_{serie} I_p}{V_T}\right) - 1\right] - \left(\frac{V_p + R_{serie} I_p}{R_{sh}}\right) \cdots\cdots\cdots (1)$$

Where I_p and V_p is the output current and output voltage of a solar cell, respectively; I_{ph} is the generated current under a given irradiation; I_p is the reverse saturation current of the diode.

$V_T = \frac{nK_BT}{q}$ is the thermodynamic potential of the cell.

Where q is the charge of an electron; K_B is the Boltzmann's constant; n is the ideality factor for a p-n junction; T is the temperature of a solar cell (°K).

Conceptually, photovoltaic cells are grouped together in order to form solar array. The relationship between the PV array output current and voltage is given by [2].

$$I_{pv} = N_p I_{ph} - N_p I_s\left\{\exp\left[\frac{q}{nKT}\left(\frac{V_{pv}}{N_s} + \frac{I_{pv} R_S}{N_p}\right)\right] - 1\right\} -$$

$$- \frac{N_p}{R_{sh}}\left(\frac{V_{pv}}{N_s} + \frac{I_{pv} R_S}{N_p}\right) \cdots\cdots \quad (2)$$

Where $I_{pv} = Np * Ip$ is current delivered by the Np cells of parallel generators; $Vpv = Ns * Vp$ is the voltage produced across the photovoltaic generator composed to Ns series cells.

In the following table are shown the characteristics of PV panel 135 W brand used in our work.

TABLE I
PHOTOVOLTAIC MODULE PARAMETRES

$P_{opt} = 135Wc$	$I_{opt} = 7,39A$	$V_{opt} = 17,6V$
$V_{co} = 21,9V$	$I_{cc} = 8,02A$	$Ns = 72Cells$

The waveform in Fig. 3 shows the effect of the illumination on $V_{PV} = f(P_{PV})$ characteristic of our photovoltaic generator.

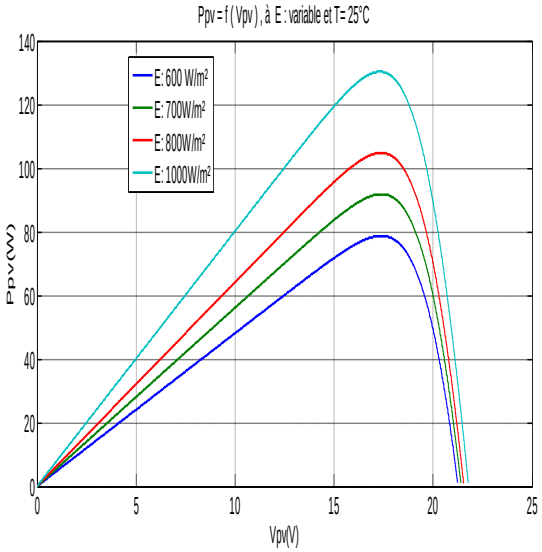

Fig. 3. Variation of the GPV power and voltage, for different values of the illumination at fixed temperature

B. *Maximum Power Point Tracking Algorithm*

The photovoltaic voltage and current can represent the maximum power point (MPP). The photovoltaic voltage is a preferable control variable because [9]:

- The temperature range variation of the photovoltaic cell is very limited
- The irradiation variation significantly affect the photovoltaic cell current, however this irradiation doesn't have impact on cell tension.

Many maximum power point tracking techniques for photovoltaic system have been developed to maximize the produced energy and a lot of these are well established in the literature. starting with simple techniques as the perturbation and observation (P&O) technique or the incremental conductance, Recently, FLC has been introduced in the tracking of the MPP .They have the advantage of being robust and relatively simple to design, they do not require, on the other hand ,complete knowledge of the operation photovoltaic system by the designer [10].

In our case, the recommended control is the Least Square method which presents rapid response. This is based on the measurement of the illumination as the set-point variable for generating the duty cycle required to the converter which generates thereafter the output power adequate. The equation that manages the MPPT method is as follows:

$$P_{ref} = c_6 V_{ref}^{\ 6} + c_5 V_{ref}^{\ 5} + c_4 V_{ref}^{\ 4} + c_3 V_{ref}^{\ 3} + c_2 V_{ref}^{\ 2} + c_1 V_{ref} + c_0 \quad (3)$$

The following figure shows the MPP trajectory for different irradiation values:

ISSN 2356-5608

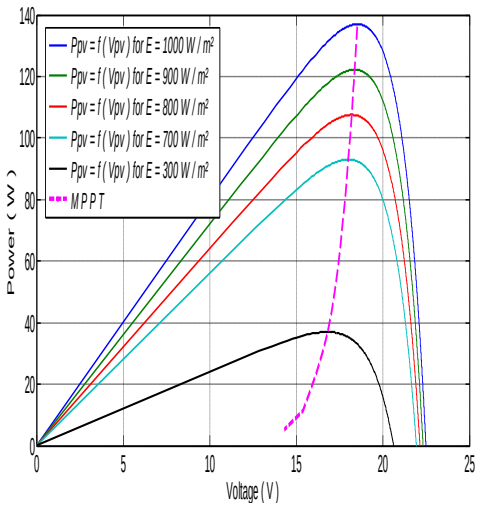

Fig. 4. Trajectory of Maximum Power Point of the Photovoltaic generator

C. DC/DC Converter Model

In stand-alone photovoltaic power systems, the output voltage is effectively a constant DC bus due to the slow dynamics of the batteries [9].

Fig.5 presents the topology of the battery storage photovoltaic system:

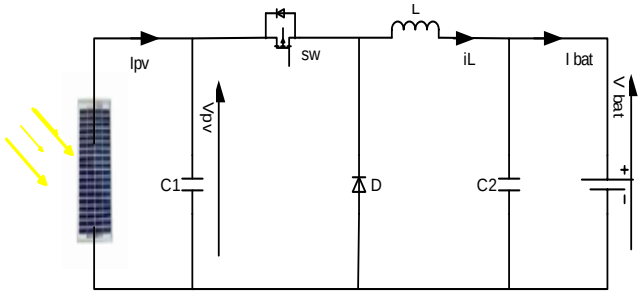

Fig 5. Topology of the energy storage system

The buck converter operates as the power interface between the photovoltaic module and load (battery). Ts and d denotes respectively the switching period and the controlled duty ratio. Fig. 6 shows the control signals of the switch SW

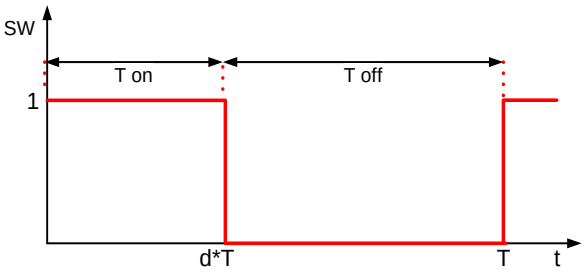

Fig. 6. Switch waveform of the converter

There is two stages, first SW=1 and second SW=0

1) Average model of DC/DC converter

To model the converter we choose two state variables including capacitor voltage $Vbat(t)$ and inductor current $iL(t)$. The system state space representation is

$$\dot{x} = A\,x + B\,u$$
$$y = Cx + Du \quad (4)$$

Where:

u is the input vector, y is the output vector and x is the status variables vector. $[iL, Vbat]^T$, $u = Vpv$ and $y = Vbat$

- During the first stage [0 , dT] the equivalent system topology is as follows

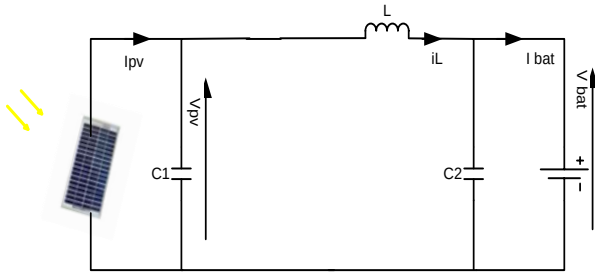

Fig. 7. Equivalent circuit (stage 1)

If we apply Kirchhoff's law

$$\frac{di_L}{dt} = \frac{Vpv}{L} - \frac{d}{L} \quad (5)$$

$$\frac{dVbat}{dt} = \frac{1}{C} * i_L - \frac{1}{C} \quad (6)$$

Spaces of states of the matrix are written as following:

$$\begin{bmatrix} \frac{di_L}{dt} \\ \frac{dVbat}{dt} \end{bmatrix} = \begin{bmatrix} 0 & \frac{-d}{L} \\ \frac{d}{C} & 0 \end{bmatrix} \begin{bmatrix} i_L \\ Vbat \end{bmatrix} + \begin{bmatrix} \frac{d}{L} & 0 \\ 0 & \frac{-d}{C} \end{bmatrix} \begin{bmatrix} Vpv \\ Ibat \end{bmatrix} \quad (7)$$

In this interval, the state space model and matrices are:

$\dot{x} = A_1 x + B_1 u$ and $y = C_1 x$

with

$$A_1 = \begin{bmatrix} 0 & -\frac{d}{L} \\ \frac{d}{C} & 0 \end{bmatrix},\ B_1 = \begin{bmatrix} \frac{d}{L} & 0 \\ 0 & -\frac{d}{C} \end{bmatrix} \text{ and } C_1 = \begin{bmatrix} 0 \\ 1 \end{bmatrix}^T$$

- During the second stage [dT, T], the equivalent system topology is as follows:

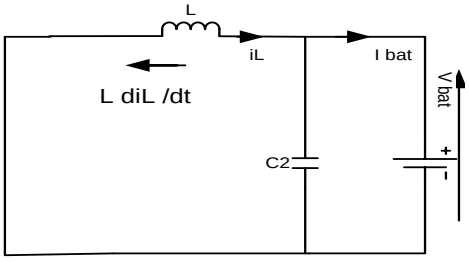

Fig. 8. Equivalent circuit (stage 2).

ISSN 2356-5608

If we apply Kirchhoff's law

$$\frac{di_L}{dt} = -\frac{Vbat}{L} \quad \text{and} \quad Ibat = \frac{I_{PV}}{d} \tag{8}$$

Spaces of states of the matrix are written as following:

$$\begin{bmatrix} \frac{di_L}{dt} \\ \frac{dVbat}{dt} \end{bmatrix} = \begin{bmatrix} 0 & \frac{d-1}{L} \\ \frac{1-d}{C} & 0 \end{bmatrix} \begin{bmatrix} i_L \\ Vbat \end{bmatrix} + \begin{bmatrix} 0 & 0 \\ 0 & \frac{d-1}{C} \end{bmatrix} \begin{bmatrix} Vpv \\ Ibat \end{bmatrix} \tag{9}$$

In the interval, the state space model and matrices are:

$\dot{x} = A_2 x + B_2 u$ and $y = C_2 x$

$$A_2 = \begin{bmatrix} 0 & \frac{d-1}{L} \\ \frac{1-d}{C} & 0 \end{bmatrix}, B_2 = \begin{bmatrix} 0 & 0 \\ 0 & \frac{d-1}{C} \end{bmatrix} \text{ and } C_2 = \begin{bmatrix} 0 \\ 1 \end{bmatrix}^T$$

Finally, the averaged model state equation can be obtained

$$\dot{x} = A\,x + B\,u \tag{10}$$

$$y = Cx$$

Where

$$A = dA_1 + (1-d)A_2 = \begin{bmatrix} 0 & \frac{-d^2+d-1}{L} \\ \frac{d^2-d+1}{L} & 0 \end{bmatrix}$$

$$B = dB_1 + (1-d)B_2 = \begin{bmatrix} \frac{d^2}{L} & 0 \\ 0 & \frac{d}{C} \end{bmatrix}$$

$$C = dC_1 + (1-d)C_2 = \begin{bmatrix} 0 \\ 1 \end{bmatrix}^T$$

2) Dynamic response of the DC/DC converter

The elaborated model is simulated in Matab/Simulink with the following parameters:

TABLE II
SIMULATIONS PARAMETER

$Vpv_{opt} = 17,6V$ FOR $E = 1000W/m^2$ and $T = 298°K$	
$Vbat = 12V$,	$C = 55\mu F$, $L = 120\mu H$, D = 0.68

Fig. 9, Shows the dynamic behaviour of the converter when a change of illumination occurs. We notice that the output voltage to the DC/DC converter requires 10 milliseconds to stabilize. This result allows us to discern that this converter can provide both high-precision.

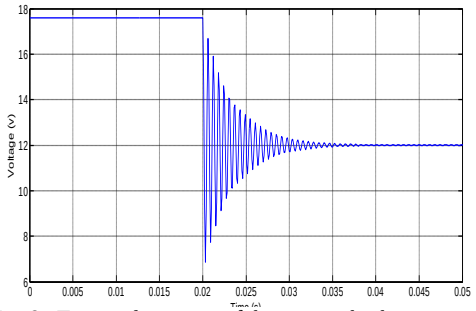

Fig. 9. Temporal response of the average back converter

D. Battery Model

A parameterized dynamic model used to represent most popular type of rechargeable battery.[7]. The equivalent circuit of the battery is shown below:

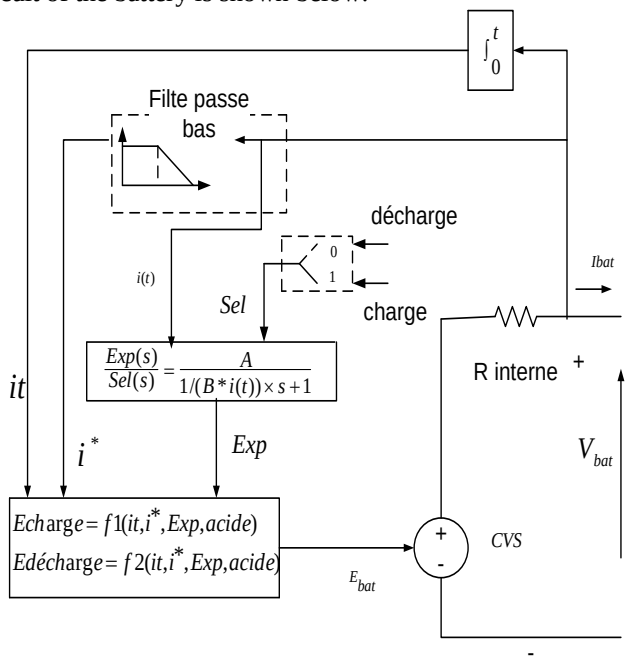

Fig. 10 Battery model lead acid type

The relationship governing the charging and discharging of this battery are given by next equations:

- Discharge Model $(i^* \succ 0)$

$$f_1(it, i^*, i, Exp) = E_0 - K\frac{Q}{Q-it}\,i^* - K\frac{Q}{Q-it}\,it + Laplace^{-1}\left[\frac{Exp(s)}{Sel(s)} \times 0\right] \tag{11}$$

- Charge Model $(i^* \prec 0)$

$$f_2(it, i^*, i, Exp) = E_0 - K\frac{Q}{it + 0{,}1 \times Q}\,i^* - K\frac{Q}{Q-it}\,it + Laplace^{-1}\left[\frac{Exp(s)}{Sel(s)} \times \frac{1}{s}\right] \tag{12}$$

ISSN 2356-5608

Where:

E_{bat} = Nonlinear voltage (V), E_0 = Constant voltage (V)

$Exp(s)$ = Exponential zone dynamics (V)

$Sel(s)$ = Represents the battery mode. $Sel(s)=0$ during battery discharge, $Sel(s)=1$ during battery charging

K = Polarization constant (Ah^{-1}) or Polarization resistance $(Ohms)$

i^* = Low frequency current dynamics (A)

i = Battery current (A)

it = Extracted capacity (Ah)

Q = Maximum battery capacity (Ah)

A = Exponential voltage (V)

B = Exponential capacity (Ah^{-1})

The parameters of the equivalent circuit can be modified to represent a particular battery type, based on its discharge characteristics.

A typical discharge curve is composed of three sections, as shown in the fig.11. The first section represents the exponential voltage drop when the battery is charged. Depending on the battery type, this area is more or less wide. The second section represents the charge that can be extracted from the battery until the voltage drops below the battery nominal voltage. The third section represents the total discharge of the battery, when the voltage drops rapidly.

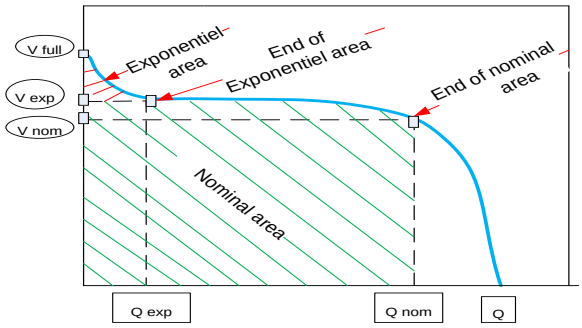

Fig. 11 Typical discharge characteristics

In our case, we used a lead acid battery whose characteristics are illustrated in the following table:

TABLE.III.

BATTERY PARAMETER

Nominal voltage battery	$V_n = 12V$
Nominal capacity battery	$Q_{\max} = 100Ah$
Full charged voltage	$Vfull = 13V$
internal resistance battery	$r_n = 0,0012\Omega$

III. Long Term Performance Test

This test aims to investigate the efficiency of our average model converter for solar charger applications and the effectiveness MPPT method during an unstable irradiation day. This test is done with following data:

- The signal of experimental measurement, illustrated in Fig. 12, is processed with Matlab software under of samples 15 milliseconds

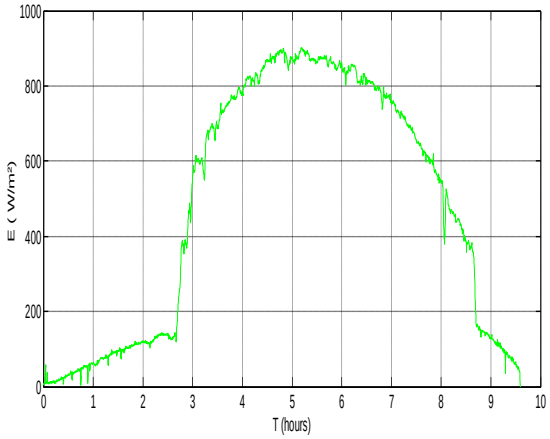

Fig. 12. Variation of the illumination during a day in Tunis (Tunisia) on 05 April 2012 [2]

- In our case, the solar irradiation not exceeded 900W / m², consequently, the PV module of the brand KYOCERA 135W does not exceed 110W

The simulations results illustrated by Figs. 13, 14, 15 and 16 show that: the duty cycle change which control the converter is proportional the change of solar irradiation. This converter operate at maximum power points, it presents no power loss as shown in Fig. 14. The maximum power generated by the panel is transferred to the battery. The difference which appeared in Fig. 15 is due to the voltage drop caused by the internal resistance of the load. The changes of battery characteristics (I_{bat} , V_{bat} , SOC) and the same of GPV (P_{PV}) proportionally with the variable illumination shows the efficiency and the performance of this average model of the DC/DC converter and also the control method used. As an addition, the simulated data was analysed to calculate the efficiency of converter, which was calculated based on energy extracted by converter and the energy stored in the battery. It was evaluated at 91%.

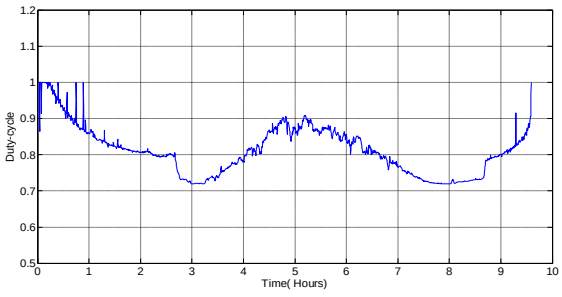

Fig. 13. Duty cycle variation

ISSN 2356-5608

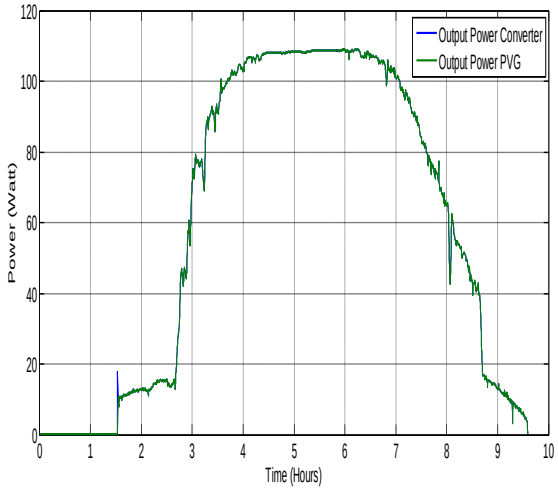

Fig. 14. Output power of the converter and power output of the photovoltaic generator

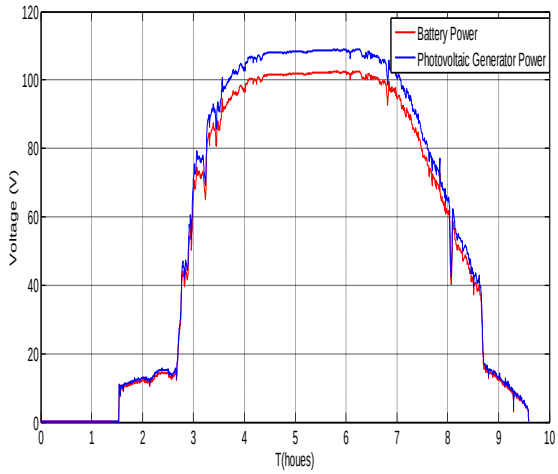

Fig. 15. Variations of the GPV power and the power battery as a function time

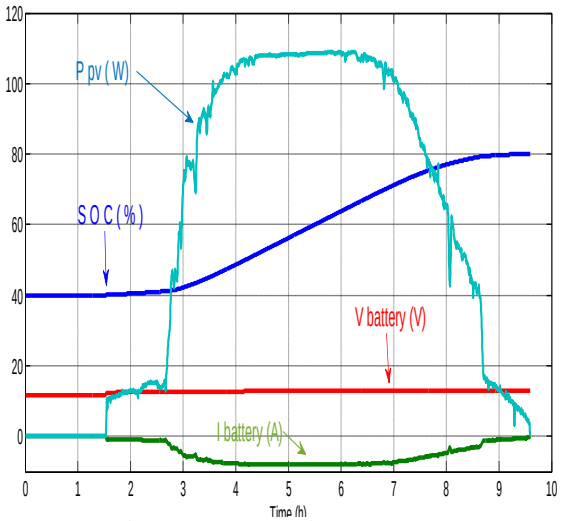

Fig. 16. Variations of the characteristics of the battery and the GPV power

IV. Conclusion

The studies of this DC/DC converter based on a new average model and his control which based on the least squares method are developed in this paper in order to optimize the power to our photovoltaic battery- storage system. This new model is an average buck converter based on state matrices, in which the energy loss is not present. This proposed control method is to adjust the output voltage in changing duty cycle, in which the response time is rapid.

The simulations results confirm the high performances for optimization to energy transfer for this photovoltaic battery-storage system.

References

[1] L. Abbassen, N. Benamrouche, M. Ounnadi, and R. Saraoui, "Modélisation et Commande d'un Système Photovoltaïque Connecté au Réseau Electrique," ICRE'2012 – 15/16 avril 2012

[2] N. Kemali, and F. Bacha , "A Maximum Power Point Tracking Algorithm Applied for Photovoltaic Water-Pumping System," 978-1-4799-2195-9/14/$31.00 ©2014 IEEE.

[3] Y. Oueslati, A. Sellami, F. Bacha and R. Andoulsi,"Sliding mode control of a photovoltaic grid connected system ", Proceedings of the 2007 International Conference on Electrical Engineering Design and Technologies (ICEEDT), November 4-6, 2007, Hammamet, Tunisia.

[4] Weidong Xiao, Nathan Ozog, and William G. Dunford, "Topology Study of Photovoltaic Interface for Maximum Power Point Tracking," IEEE Transactions On Industrial, Electronics, vol 54, no 3, Juan 2007.

[5] Olivier Tremblay1, Louis-A. Dessaint, "Experimental Validation of a Battery Dynamic Model for EV Applications," *World Electric Vehicle Journal Vol. 3 - ISSN 2032-6653 - © 2009 AVERE*

[6] M. El Ouariachi, T. Mrabti, M.F. Yaden, Ka. Kassmi and K. Kassmi, "Analysis, optimization and modeling of electrical energies produced by the photovoltaic panels and systems," *Revue des Energies Renouvelables Vol. 14 N°4 (2011) 707 – 716.*

[7] Chihchiang Hua and Jong Rong Lin, "DSP-Based Controller Application in Battery Storage of Photovoltaic System," 0-7803-2775-619$64 .000 1996 IEEE.

[8] Patil A, Atar K, Potdar A, and Mudholkar R, "embedded fuzzy module for battery charger control," IJAREEIE- Vol. 2, Issue 8, August 2013-ISSN (Online): 2278 – 8875

[9] Weidong Xiao, Nathan Ozog, and William G. Dunford, "Topology Study of Photovoltaic Interface for Maximum Power Point Tracking," IEEE Transactions On Industrial, Electronics, vol 54, no 3, Juan 2007.

[10] M. Amari, J. Ghouili, and F. Bacha , "Avrage Model of a High Frequency DC/DC Converter for Fuel Cell Application in Electrical Vehicule," International Conference on Control, Engineering & Information Technology (CEIT'13), Proceedings Engineering & Technology - Vol.1, pp. 115-121, 2013.

ISSN 2356-5608